

Textile antenna integrated with compact AMC and parasitic elements for WLAN/WBAN applications

Herwansyah Lago¹ · Ping Jack Soh^{1,2}  · Mohd Faizal Jamlos^{1,3} · Nursuriati Shohaimi¹ · Sen Yan² · Guy A. E. Vandenbosch²

Received: 16 June 2016 / Accepted: 17 November 2016 / Published online: 29 November 2016
© Springer-Verlag Berlin Heidelberg 2016

Abstract A wearable antenna fully designed and fabricated using textile is presented. Both antenna and artificial magnetic conductor plane are designed for operation in the wireless local area network (WLAN)/wireless body area network (WBAN) band from 2.4 to 2.5 GHz. The AMC unit element is designed based on the rectangular patch structure, which is then integrated using slots and slits for bandwidth broadening. Meanwhile, the combination of the slits and L-shaped parasitic elements applied at four edges of the rectangular antenna structure enabled unidirectional radiation outwards from the body. The structure is coaxially fed using a rectangular ring slot centered on the radiating element. Simulated and measured reflection and radiation performance indicate a satisfactory agreement, fulfilling the requirements for WLAN/WBAN applications both in free space and on body. The shielding effectiveness provided by the AMC plane is also evaluated numerically in terms of specific absorption rate, indicating levels below the European regulatory limit of 2 W/kg.

1 Introduction

In recent years, wearable systems are becoming increasingly significant due to their promising features in applications such as tracking, navigation, mobile computing and public safety: conformity, flexibility and ease of use. Besides being spurred by the recent standardization of Body Area Networks (BANs) via IEEE 802.15.6, research in wearable systems is becoming popular also due to the ease of integration on the human body. One of the main components of such systems is the antenna, which is most suitable to be realized using textiles or other flexible materials.

The application of wearable antennas requires them to be located close to the human body. Due to the lossy nature of the human body, electromagnetic interaction with the antenna must be minimized. A high front-to-back ratio (FBR) of the radiation is beneficiary to reduce this interaction. A popular method to realize this is to ensure that the chosen planar antenna topology features a ground plane between the antenna and human body to avoid the absorption of large amounts of radiated power, besides affecting the matching due to coupling. In addition to that, electromagnetic power absorbed by the body may present a health risk factor. This is quantified by the specific absorption rate (SAR), the power absorbed per unit mass.

To enable a high FBR, electromagnetic band gap (EBG) structures have been suggested in the literature [1, 2]. However, such antennas embedded with vias potentially produce distorted radiation patterns [3]. Yan [4], Zhang [5], Rahim [6], Prakash [7] and Yang [8] have demonstrated the enhancement of the antenna performance using an artificial magnetic conductor (AMC). An AMC plane is a type of two-dimensional metasurface which is widely used for

✉ Ping Jack Soh
pjsoh@unimap.edu.my; pingjack.soh@esat.kuleuven.be

¹ Advanced Communication Engineering (ACE) CoE, School of Computer and Communication Engineering, Universiti Malaysia Perlis (UniMAP), Pauh Putra Campus, 02600 Arau, Perlis, Malaysia

² ESAT-TELEMIC Research Division, KU Leuven, Kasteelpark Arenberg 10, Box 2444, 3001 Leuven, Belgium

³ Faculty of Mechanical Engineering, Universiti Malaysia Pahang (UMP), Pekan, Pahang, Malaysia

planar antennas [9, 10]. In addition, an AMC plane can be placed close to the radiator [4, 5].

In this work, a slotted microstrip antenna backed by an AMC plane is proposed for WLAN applications. The AMC plane is designed based on a slotted rectangular structure to ensure compactness. Compared to the previous literature, this work features a relatively compact AMC unit cell sized at $50 \times 50 \text{ mm}^2$, which is about $0.4 \times 0.4 \lambda$ for operation at 2.4 GHz. In contrast, previous work mainly concentrated on implementing simpler rectangular structures due to the larger fabrication tolerance when using textiles [4, 11]. It is also demonstrated that the AMC is effective in isolating the main radiator from the body. Besides that, the proposed AMC layer is also validated to be capable of reducing the antenna front-to-back ratio (FBR), gain improvement and bandwidth enhancement. The next section first describes the AMC topology, materials used and performance. Next, Sect. 3 explains the radiator topology, the integration process with a 2×2 AMC plane and their performance. The free space and on-body performance are evaluated in Sect. 4 prior to the concluding remarks.

2 Design of the AMC plane

Instead of using conventional square patch structures to form the AMC, square patches with slots and slits at their edges are chosen to miniaturize the AMC size. The topology of a single AMC unit cell fully designed using textiles is illustrated in Fig. 1. The patches are placed on a 3-mm thick felt substrate with a dielectric constant and loss tangent of 1.4 and 0.044, respectively. To form the metallic layers, Shieldit Super conductive textile from LessEMF Inc. with a conductivity of $1.18 \times 10^8 \text{ S/m}$ is used. Another layer of substrate and a layer of ground are located at the reverse side of the AMC layer to complete the AMC plane. Besides that, a top substrate is used to separate the AMC plane from the antenna. As shown in Fig. 2, the phase of the reflected wave is about 0° for 2.45 GHz, which demonstrates the PMC-like characteristic. The operating bandwidth of the AMC plane, defined by a $\pm 90^\circ$ phase response, is from 2.24 to 2.51 GHz.

3 Antenna on AMC plane

The overall antenna topology is depicted in Fig. 3. The main radiator consists of a square patch with C-shaped notches in the middle of each of the edges. A rectangular ring slot is positioned centrally and fed using a 50Ω SMA coaxial connector. Note that the notches, ring and L-shaped elements in the corners enable miniaturization of the

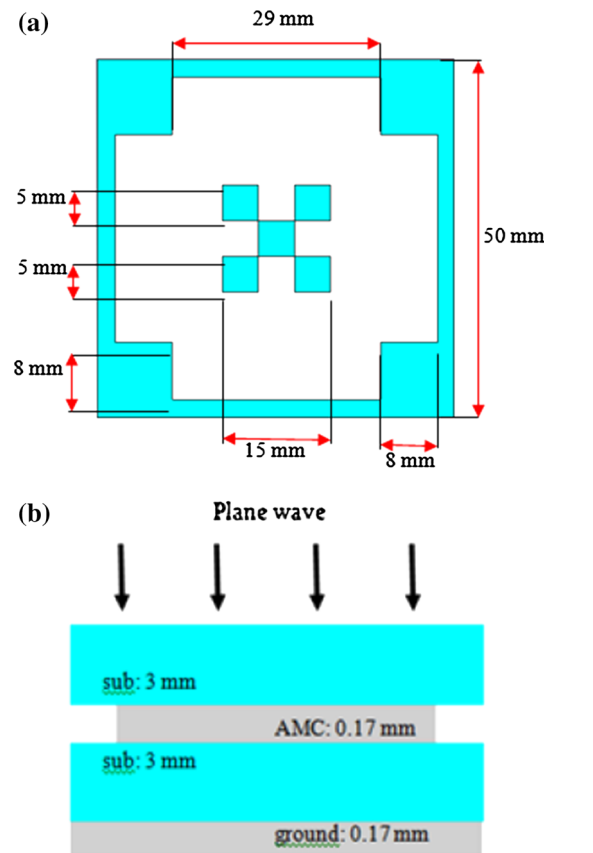


Fig. 1 AMC unit cell topology. **a** AMC dimensions, **b** side view

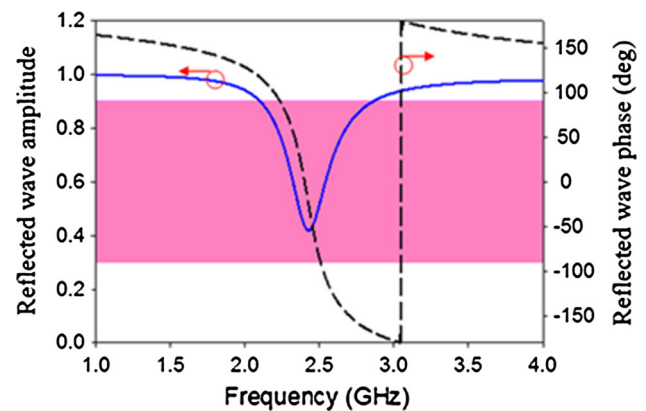


Fig. 2 Simulated performance of the AMC unit cell

antenna. The final AMC-like structure consists of 2×2 elements of the AMC unit cell, see Fig. 3d.

The fabricated prototype is depicted in Fig. 3d. The simulated and measured reflection coefficients (S_{11}) are depicted in Fig. 4. The measured bandwidth is slightly smaller than the simulated one. The measured S_{11} is -12.4 dB , and the simulated S_{11} is -15.65 dB at the desired frequency of 2.45 GHz. This small disagreement is caused by the larger fabrication tolerances as simple manual tools

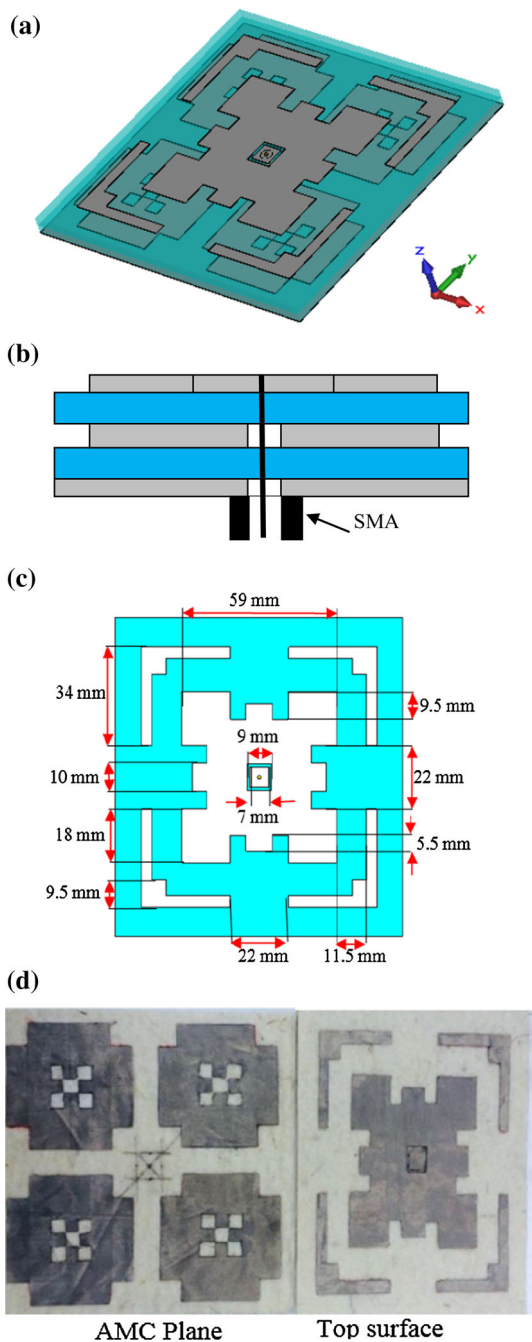


Fig. 3 Topology of the proposed antenna. **a** 3-D view, **b** side view, **c** top view, **d** fabricated prototype

were used to fabricate the antenna, and by the uncertainties concerning the material properties. However, the prototype meets the requirements for WLAN communications.

The simulated and measured radiation patterns at 2.45 GHz are shown in Fig. 5. The antenna beams are pointed toward four main directions: two of them in the xz -plane and others at yz -plane. The difference between co- and cross-polarization for both planes is more than 60 dB at all directions. This is due to feeding position and slit rectangular with the

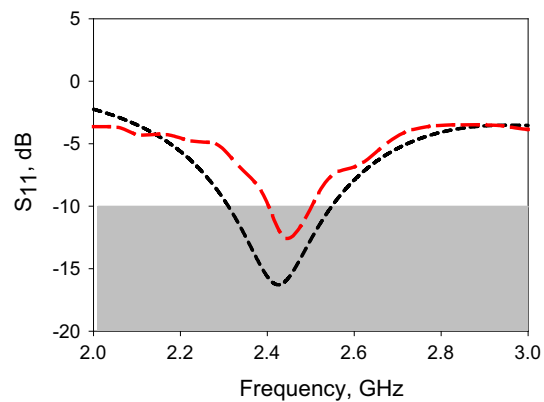


Fig. 4 Simulated and measured reflection coefficients in free space (long red dashed line measured, short black dashed simulated)

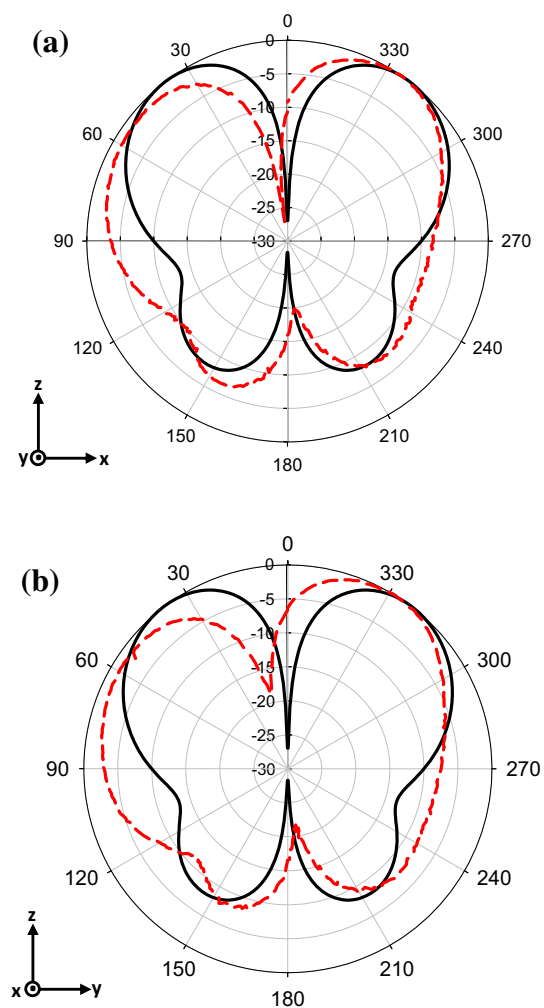


Fig. 5 Radiation patterns at 2.45 GHz, **a** xz -plane, **b** yz -plane (solid black line simulated, dashed red line measured)

presence of the L-shaped parasitic at the edges and fulfills the WBAN requirement with a multi-beam direction [12, 13]. The maximum realized gain and bandwidth of the antenna are

about 2.42 dB and 9.85% at 2.45 GHz, respectively, while its total efficiency is more than 40% at 2.45 GHz, which is typical for textile antennas fabricated using these materials [14]. The presence of the AMC plane contributed to the improved performance. When a normal ground is applied to the antenna without the AMC layer, a lower gain and bandwidth of 0.41 dB and 5.53% are obtained at 2.45 GHz, while the total efficiency is also lower than 40%.

4 Performance on body

The antenna was simulated on two human body models: a simplified model consisting of three layers (skin, fat and muscle) and a more detailed model, the Hugo voxel model.

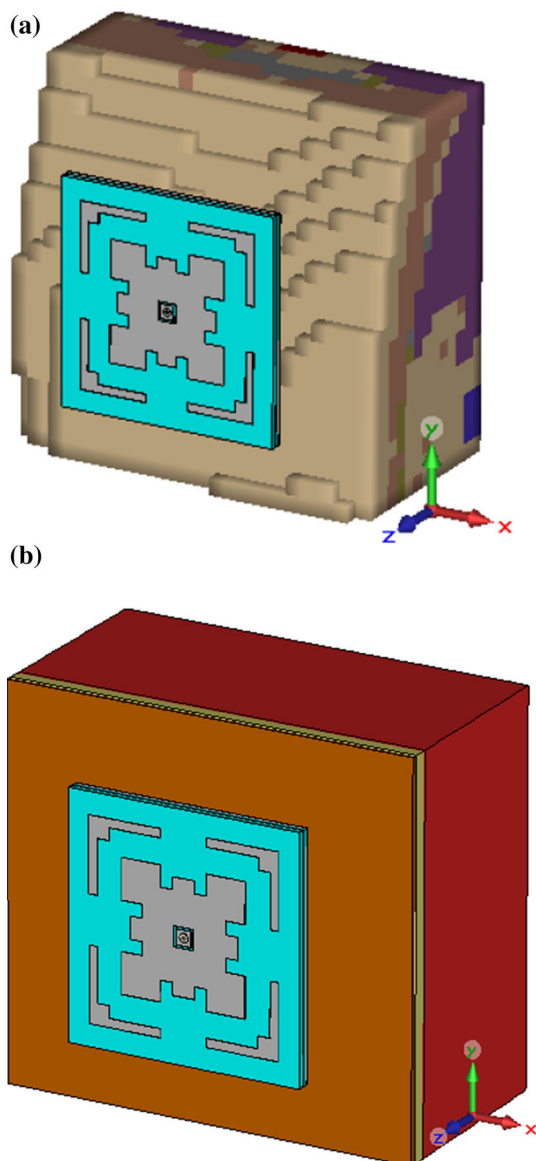


Fig. 6 Antenna placement on the **a** truncated detailed human body model and **b** simple human model

The simple model is depicted in Fig. 6b. It represents the human chest and was validated in [4, 14]. The detailed model involves a cutout of the chest obtained from the full body Hugo model, see Fig. 6a.

The antenna is positioned on the models with a distance of 15 mm between the body model and the antenna ground. Due to the presence of the ground plane, the simulated S_{11} for both models is very similar to the S_{11} simulated in free space, see Fig. 7. At 2.45 GHz, the minimum S_{11} is -14.07 and -17.34 dB when simulated on the detailed and the simple model, respectively.

The prototype was also measured at least three times in an anechoic chamber while positioned on the chest of several human volunteers, as tabulated in Table 1. The averaged results are shown in Fig. 7. Most of the measurement results agree with the simulations using both models. The larger disagreements for volunteers 1 and 2 may be due to the difficulty in accurately positioning the antenna at a fixed distance from the subject in practice. Nonetheless, this evaluation indicates that the antenna fulfills the requirements for WLAN communications when operated on the human chest.

To further evaluate the effectiveness of the AMC plane in minimizing backward radiation, the specific absorption rate (SAR) and radiation pattern were evaluated. This was done numerically using the detailed human body model in CST Microwave Studio. The input power to the antenna was set at 0.5 W, and the SAR was calculated based on the IEEE/IEC 6270-1 standard, averaged to 10 g of biological tissue. The SAR distribution is displayed in Fig. 8a. Note

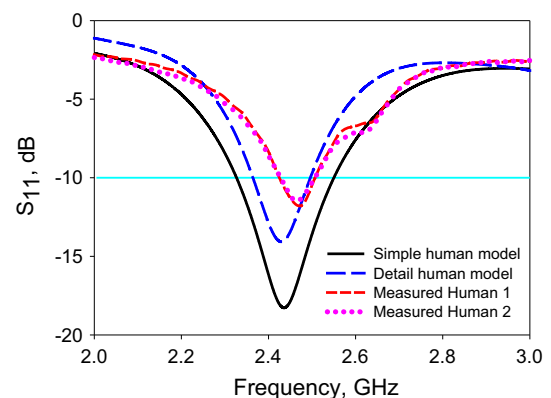


Fig. 7 Simulated and measured reflection coefficients (S_{11}) of the antenna operating on the chest

Table 1 Details of the volunteers involved in the measurements

Volunteer no.	Gender	Height (cm)	Weight (kg)
1	Female	157	60
2	Female	163	68

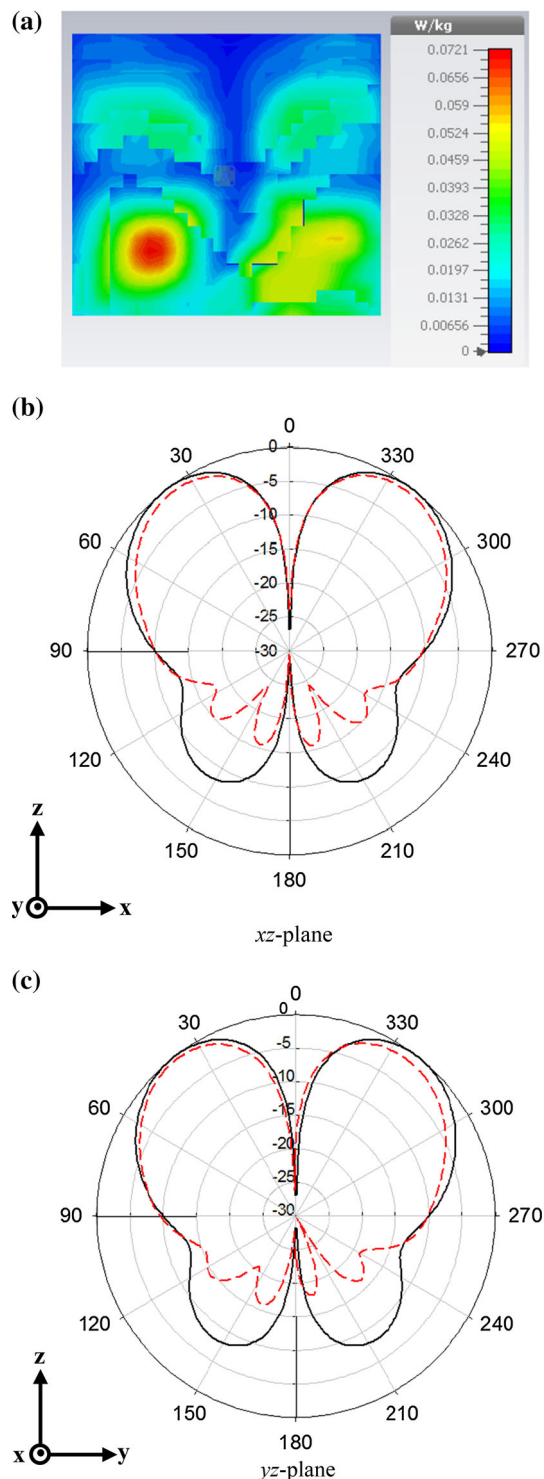


Fig. 8 Simulated **a** SAR distribution and **b** radiation pattern comparison of the antenna placed on the detailed human body model (dashed red line) and free space (solid black line) at 2.45 GHz

that the maximum SAR produced in the detailed human model is only 0.0721 W/kg, which is much lower than the regulatory limit of 2 W/kg. The difference between the radiation patterns evaluated in free space and the detailed

human body model is shown in Fig. 8b. The difference between co- and cross-polarized components for the on-body pattern is 27.62 dB (not shown in the figure). Furthermore, the maximum on-body gain in both planes is lowered to 2.22 dB at 2.45 GHz due to the absorption by human body.

5 Conclusions

In this paper, a miniaturized AMC-integrated all-textile antenna for WLAN/WBAN applications was proposed. This novel structure combines a patch antenna incorporated with slots and slits to ensure miniaturization. Moreover, its combination with the L-shaped parasitic elements located at its corners to enable radiation outward from the body. Suppressed backward radiation and reduced front-to-back ratio are ensured by the placement of an all-textile AMC plane. Effectively resulting in a reduced electromagnetic coupling with the body, it ensures a low SAR level of 0.0721 W/kg, which is far below the regulatory limit of 2 W/kg. Simulations and measurements performed in free space and on body are in good agreements, satisfactory fulfilling the requirements for WLAN/WBAN applications.

Acknowledgements This project is supported by the Fundamental Research Grant Scheme (FRGS) (Grant No. 9003-00527) and Universiti Malaysia Perlis Incentive Grant (Grant No. 9007-00177). Herwansyah Lago is supported by the MyBrain15 Scholarship from the Malaysian Ministry of Higher Education (MOHE). The authors would like to acknowledge Fatin Nabilah Gimam and Ezzatyy Faridah Nor for their assistance.

References

1. L. Akhondzadeh-Asl, D.J. Kern, P.S. Hall, D.H. Werner, Wideband dipoles on electromagnetic bandgap ground planes. *IEEE Trans. Antennas Propag.* **55**(9), 2426–2434 (2007)
2. S. Zhu, R. Langlely, Dual-band wearable textile antenna on an EBG substrate. *IEEE Trans. Antennas Propag.* **57**(4 part 1), 926–935 (2009)
3. S.R. Best, D.L. Hanna, Design of a broadband dipole in close proximity to an EBG ground plane. *IEEE Antennas Propag. Mag.* **50**(6), 52–64 (2008)
4. S. Yan, P.J. Soh, G.A.E. Vandenbosch, Low-profile dual-band textile antenna with artificial magnetic conductor plane. *IEEE Trans. Antennas Propag.* **62**(12), 6487–6490 (2014)
5. Y. Zhang, J. Von Hagen, M. Younis, C. Fischer, W. Wiesbeck, Planar artificial magnetic conductors and patch antennas. *IEEE Trans. Antennas Propag.* **51**(10I), 2704–2712 (2003)
6. M.K.A. Rahim, N.A. Samsuri, K. Kamardin, P.S. Hall, Vertical and horizontal transmission enhancement between antennas using textile artificial magnetic conductor waveguide sheet. *Electron. Lett.* **51**(9), 671–673 (2015)
7. P. Prakash, M.P. Abegaonkar, S. Member, A. Basu, S.K. Koul, Gain enhancement of a CPW-fed monopole antenna using polarization-insensitive AMC structure. *IEEE Antennas Wirel. Propag. Lett.* **12**, 1315–1318 (2013)

8. W.C. Yang, H. Wang, W.Q. Che, Y. Huang, J. Wang, High-gain and low-loss millimeter-wave LTCC antenna array using artificial magnetic conductor structure. *IEEE Trans. Antennas Propag.* **63**(1), 390–395 (2015)
9. D. Sievenpiper, L. Zhang, R.F. Jimenez Broas, N.G. Alexopoulos, E. Yablonovitch, High-impedance electromagnetic surfaces with a forbidden frequency band. *IEEE Trans. Microw. Theory Tech.* **47**(11), 2059–2074 (1999)
10. F. Yang, Y. Rahmat-Samii, Reflection phase characterizations of the EBG ground plane for low profile wire antenna applications. *IEEE Trans. Antennas Propag.* **51**(10), 2691–2703 (2003)
11. O. Folayan, R. Langley, Dual frequency band antenna combined with a high impedance band gap surface. *IET Microw. Antennas Propag.* **3**(7), 1118 (2009)
12. P.J. Soh, G.A.E. Vandenbosch, S.L. Ooi, M.R.N. Husna, Wearable dual-band Sierpinski fractal PIFA using conductive fabric. *Electron. Lett.* **47**(6), 365 (2011)
13. J.G. Santas, A. Alomainy, Y. Hao, Textile antennas for on-body communications: techniques and properties. *The Second European Conference on Antennas and Propagation (EuCAP), Edinburgh (2007)*, pp. 1–4
14. S.J. Boyes, S. Member, P.J. Soh, Y. Huang, S. Member, G.A.E. Vandenbosch, N. Khiabani, Measurement and performance of textile antenna efficiency on a human body in a reverberation chamber. *IEEE Trans. Antennas Propag.* **61**(2), 871–881 (2013)